Progress Towards an Order of Magnitude Improvement on the Measurement of the Electron Electric Dipole Moment

ACME Collaboration: Daniel Ang,[1] David DeMille[2] (PI), John M. Doyle[1] (PI), Gerald Gabrielse[1] (PI), Jonathan Haefner,[1] Zack Lasner,[2] Cole Meisenhelder,[1] Cristian Panda,[1] Adam West,[2] Elizabeth P. West,[1] Xing Wu[2]
Affiliation: [1]Harvard University, [2]Yale University

Motivation & Theory

$$H_d = -\vec{d}_e \cdot \vec{\mathcal{E}}$$

Permanent EDMs violate T-symmetry. Many theories beyond the Standard Model predict T violation and EDMs at current experimental precision.

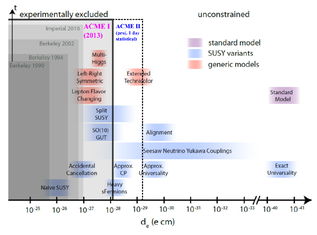

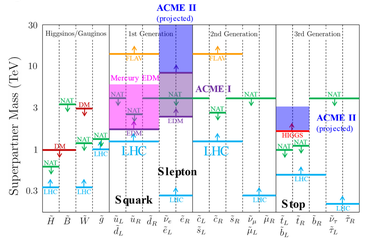

Figure taken from Feng (2013)

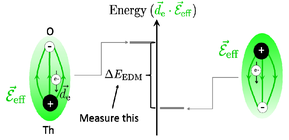

$$\delta d_e = \frac{\hbar}{2C\tau\mathcal{E}_{\text{eff}}\sqrt{\dot{n}T}}$$

Effective electric field $\mathcal{E}_{eff}$: ~80 GV/cm
Precession time τ: ~1 ms
Measurement contrast C: ~0.95
Integration time T: set at ~340 hours
(Detected) molecule flux $\dot{n}$:
ACME I: ~ 3×10^4 s^{-1}
ACME II: ~ 1×10^7 s^{-1}
ACME I result: $d_e = (-2.2 \pm 4.8) \times 10^{-29}$ e · cm
$\Rightarrow |d_e| < \mathbf{9.3 \times 10^{-29}\ e \cdot cm}$
Projected ACME II sensitivity: $\boldsymbol{\delta d_e \sim 10^{-29}\ e \cdot cm}$

1. Buffer gas beam source

ThO in the gas phase is produced through **pulsed ablation of a ceramic ThO_2 target** with an Nd:YAG laser. Ablation is performed at 50 Hz in a cryogenic buffer gas cell. The ThO molecules thermalize with and are entrained in the flow of the neon buffer gas. The molecular beam is cooled to 4 K. Each pulse produces a flux of ~10^{11} molecules per steradian in the electro-vibrational ground state.

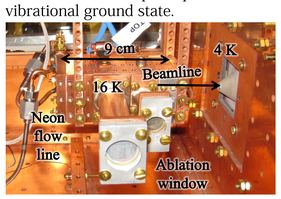

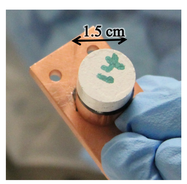

Ceramic ThO_2 ablation target

2. Rotational Cooling

The molecules in the X state are primarily distributed in the lowest four rotational states after leaving the cell. Optical pumping on the $X - C$ transition transfers population from the $J = 0, 1, 2$ levels to the $J = 0$ level, increasing usable molecule flux by a factor of ~2.7.

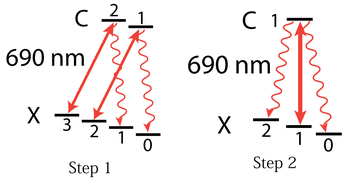

3. State Preparation

The EDM measurement is performed in the metastable H state. STIRAP **coherently transfers population** through an intermediate short-lived state to the spin-aligned state that represents the beginning of the EDM measurement. This transfer occurs with an efficiency of ~75%.

STIRAP Level Structure

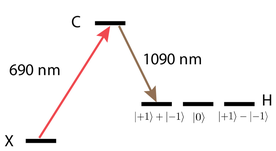

Cleanup Level Structure

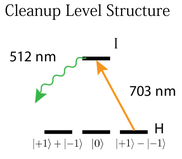

A separate 703 nm cleanup laser reprojects the spin-aligned state prepared by the STIRAP lasers onto a coherent superposition of $M = +1, M = -1$ states, suppressing possible EDM-like phases caused by the STIRAP beams.

ACME II Apparatus

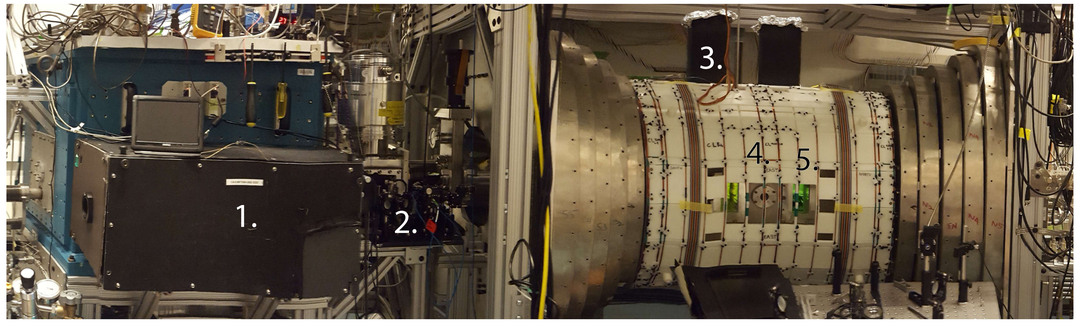

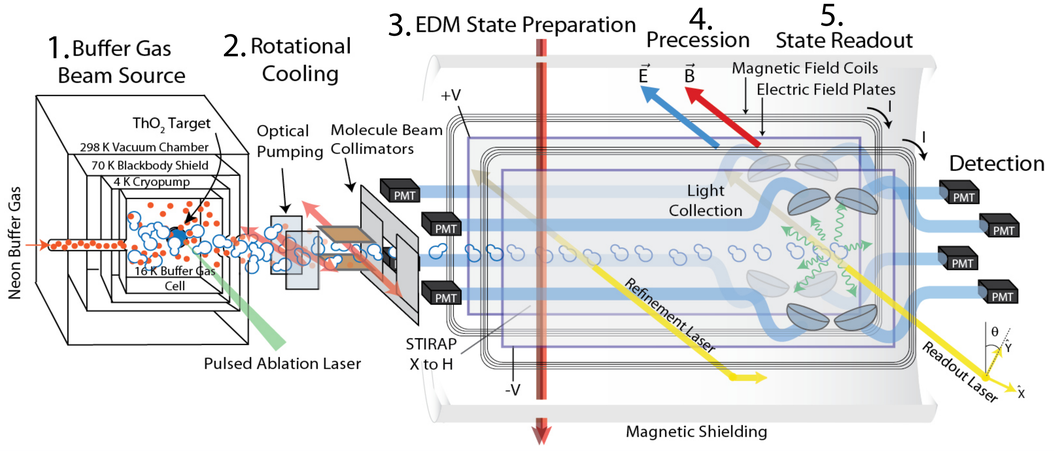

4. State Precession

The molecules in the prepared state **precess and acquire phase** as they fly through the electric and magnetic fields of the interaction region.

$$\frac{1}{\sqrt{2}}(|-1\rangle + |+1\rangle) \longrightarrow \frac{1}{\sqrt{2}}(e^{i\phi}|-1\rangle + e^{-i\phi}|+1\rangle)$$

$$\frac{\phi}{\tau} = -(\tilde{\mathcal{B}} g_1 \mu_B \mathcal{B}_z + \tilde{\mathcal{N}}\tilde{\mathcal{E}} d_e \mathcal{E}_{\text{eff}})$$

5. State Readout

At the end of the interaction region, the final state is **projected to a pair of orthogonal basis vectors** by subjecting the molecules to a 703 nm probe laser (on the H-I transition) with linear polarization rapidly switched (200 kHz) between x and y.

We **collect the 512 nm fluorescence** using PMTs as the molecules in the short-lived I-state decay back to the ground state.

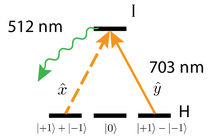

Data Acquisition Structure

The spin precession is performed with different configurations of parameters that switch the sign of the different terms that contribute to the phase.

This enables us to **extract the EDM contribution to the phase** by performing "**parity sums**" of the different phases taken under different conditions, and also diagnose and suppress known systematic errors.

By performing the experiment with different values of $\tilde{N}$, $\tilde{E}$, $\tilde{B}$ we can extract **the EDM channel $\boldsymbol{\phi^{\tilde{N}\tilde{E}}}$**, the component of the phase which is odd under reversal of $\tilde{N}$ and $\tilde{E}$.

This measurement scheme results in robust suppression of systematic effects: any imperfections in the system would have to be correlated with $\tilde{N}$ and $\tilde{E}$ to become a source of systematic error.

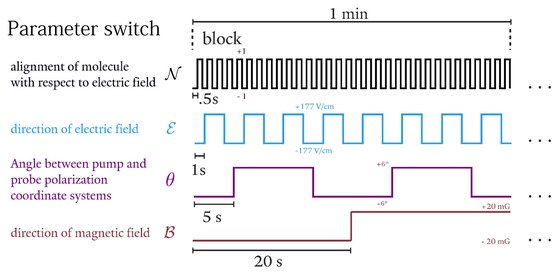

$$\phi(\tilde{\mathcal{N}}, \tilde{\mathcal{E}}, \tilde{\mathcal{B}}) = \tilde{\mathcal{N}}\phi^{\tilde{\mathcal{N}}} + \tilde{\mathcal{E}}\phi^{\tilde{\mathcal{E}}} + \tilde{\mathcal{B}}\phi^{\tilde{\mathcal{B}}} + \boxed{\tilde{\mathcal{N}}\tilde{\mathcal{E}}\phi^{\tilde{\mathcal{N}}\tilde{\mathcal{E}}}} + \tilde{\mathcal{N}}\tilde{\mathcal{B}}\phi^{\tilde{\mathcal{N}}\tilde{\mathcal{B}}} + \tilde{\mathcal{E}}\tilde{\mathcal{B}}\phi^{\tilde{\mathcal{E}}\tilde{\mathcal{B}}} + \tilde{\mathcal{N}}\tilde{\mathcal{E}}\tilde{\mathcal{B}}\phi^{\tilde{\mathcal{N}}\tilde{\mathcal{E}}\tilde{\mathcal{B}}}$$
$$\tilde{\mathcal{N}}, \tilde{\mathcal{E}}, \tilde{\mathcal{B}} \in \{+1, -1\}$$
EDM phase

Systematic Search & Characterization

Other possible sources of systematic error are checked by intentionally exaggerating various imperfections in the system and measuring their effect on the EDM channel $\omega^{\tilde{N}\tilde{E}} = \frac{\phi^{\tilde{N}\tilde{E}}}{\tau}$, where τ is the precession time.

We have checked the main contributions to systematic error budget in ACME I and confirmed that they are all suppressed to below anticipated ACME II senstivity levels. We are currently investigating secondary effects showing up in other (non-EDM) channels and continue varying system parameters, looking for possible shifts in the EDM channel.

Example: Correlation between prepared phase and power

We found a non-zero dependence of the EDM channel $\omega^{\tilde{N}\tilde{E}}$ vs applied cleanup laser power:

$$P^{app} = P^{nr}(1 + \tilde{N}\tilde{E}\frac{P^{\tilde{N}\tilde{E}}}{P^{nr}})$$

We observed that the slope depended on **the global polarization angle of the lasers**. If for some reason there turns out to be an intrinsic $P^{\tilde{N}\tilde{E}}$ **in the system, this could masquerade as an EDM.**

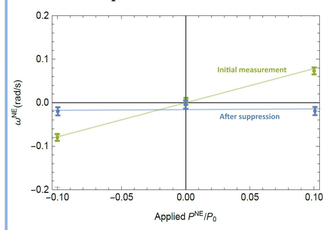

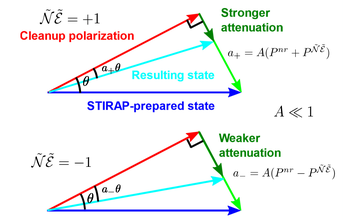

We discovered that this dependence arose from a misalignment in the angle between the initial spin state (prepared by STIRAP) and the cleanup laser polarization. The cleanup laser was not perfectly attenuating the component of the spin perpendicular to its polarization, resulting in a shift in $\omega^{\tilde{N}\tilde{E}}$ when $P^{\tilde{N}\tilde{E}}$ is applied.

With sufficient cleanup power and **tuning the global polarization angle** we are able to suppress the possible systematic error arising from this to below our anticipated ACME II sensitivity.

Statistical Gains Versus ACME I

Demonstrated upgrades	Gain (molecule flux)
Geometric factors (shorter beamline, wider field plates)	~8 ×
More efficient fluorescence collection	~2.5 ×
STIRAP state preparation (upgrade from optical pumping)	~12 ×
Higher quantum efficiency of PMTs at 512 nm detection wavelength	~2.5 ×
Total demonstrated statistical improvement (actual)	**~450 ×**

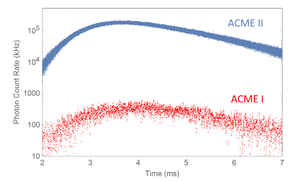

Comparison of ACME I and ACME II spin precession fluorescence data

Outlook

The ACME II measurement of the electron EDM is currently ongoing, measuring ThO spin precession with a daily statistical uncertainty of 10^{-29} e • cm.

We are currently checking for and investigating systematic effects, with the aim of a measurement near or better than 10^{-29} e • cm.

References

ACME I result: J Baron et al., *Science* **343**, p. 269-272 (2014)
ACME I detailed report: J Baron et al., arXiv:1612.09318
STIRAP state preparation: C.D. Panda et al., Phys. Rev. A **93**, 052110 (2016)
Previous eEDM Limit: J. J. Hudson et al., *Nature* **473**, 7348 (2011)
E_{eff} Calculations: L. V. Skripnikov et al., *J. Chem. Phys.* **142** 024301 (2015), T. Fleig et al., *J. Mol. Spec.* **300** p. 16-21 (2014)
EDM & SUSY: J. Feng, Annu. Rev. Nucl. Part. Sci., 63:351-82 (2013)

More information: www.electronedm.info